

# New Steady-State Quiescent High-Confinement Plasma in an Experimental Advanced Superconducting Tokamak

J. S. Hu,<sup>1,\*</sup> Z. Sun,<sup>1</sup> H. Y. Guo,<sup>1,2</sup> J. G. Li,<sup>1</sup> B. N. Wan,<sup>1</sup> H. Q. Wang,<sup>1</sup> S. Y. Ding,<sup>1</sup> G. S. Xu,<sup>1</sup> Y. F. Liang,<sup>1,3</sup>  
D. K. Mansfield,<sup>4</sup> R. Maingi,<sup>4</sup> X. L. Zou,<sup>5</sup> L. Wang,<sup>1</sup> J. Ren,<sup>1</sup> G. Z. Zuo,<sup>1</sup> L. Zhang,<sup>1</sup> Y. M. Duan,<sup>1</sup>  
T. H. Shi,<sup>1</sup> L. Q. Hu,<sup>1</sup> and East team

<sup>1</sup>*Institute of Plasma Physics, Chinese Academy of Sciences, Hefei, Anhui 230031, China*

<sup>2</sup>*General Atomics, P.O. Box 85608, San Diego, California 92186-5608, USA*

<sup>3</sup>*Forschungszentrum Jülich GmbH, Association EURATOM-FZ, Jülich D-52425, Germany*

<sup>4</sup>*Princeton University Plasma Physics Laboratory, Princeton, New Jersey 08543, USA*

<sup>5</sup>*CEA, IRFM, F-13108 Saint-Paul-lez-Durance, France*

(Received 19 August 2014; revised manuscript received 14 September 2014; published 3 February 2015)

A critical challenge facing the basic long-pulse high-confinement operation scenario (*H* mode) for ITER is to control a magnetohydrodynamic (MHD) instability, known as the edge localized mode (ELM), which leads to cyclical high peak heat and particle fluxes at the plasma facing components. A breakthrough is made in the Experimental Advanced Superconducting Tokamak in achieving a new steady-state *H* mode without the presence of ELMs for a duration exceeding hundreds of energy confinement times, by using a novel technique of continuous real-time injection of a lithium (Li) aerosol into the edge plasma. The steady-state ELM-free *H* mode is accompanied by a strong edge coherent MHD mode (ECM) at a frequency of 35–40 kHz with a poloidal wavelength of 10.2 cm in the ion diamagnetic drift direction, providing continuous heat and particle exhaust, thus preventing the transient heat deposition on plasma facing components and impurity accumulation in the confined plasma. It is truly remarkable that Li injection appears to promote the growth of the ECM, owing to the increase in Li concentration and hence collisionality at the edge, as predicted by GYRO simulations. This new steady-state ELM-free *H*-mode regime, enabled by real-time Li injection, may open a new avenue for next-step fusion development.

DOI: 10.1103/PhysRevLett.114.055001

PACS numbers: 52.40.Hf, 52.35.Ra, 52.55.Fa

Magnetic confined fusion offers one of the most promising approaches to nuclear fusion that potentially provides an environmentally friendly and intrinsically safe energy source with an abundant fuel supply. High-performance and steady-state operation is a crucial goal of current magnetic fusion research [1]. Although long-pulse plasma operation has been demonstrated in various fusion experiments [2], a great challenge facing future fusion devices is to achieve a steady-state high-confinement (*H*-mode) plasma regime with acceptable divertor heat fluxes (below 10 MW/m<sup>2</sup> for both graphite and tungsten) [3,4]. Large edge localized modes (ELMs) that typically accompany *H*-mode operation would generate an unacceptable heat load on the plasma facing components (PFCs) [5,6]. How to reduce the transient divertor peak heat load induced by ELMs is a critical issue for long-pulse *H*-mode operations. Great progress has been made over the last decade in the development of quasisteady quiescent or ELM-suppressed *H*-mode discharges in tokamaks, as well as techniques to mitigate ELMs or trigger more frequent, small ELMs, along with the associated pedestal conditions [7,8]. However, a fundamental difficulty has been encountered by researchers in this field: ELM-free *H* modes usually lead to a rapid rise in plasma density and impurity accumulation in the plasma core, which, in turn, results in unacceptably

high radiated power levels [9,10]. There are notable exceptions to this statement: the quiescent *H* mode [11,12] does not suffer from impurity accumulation, but has restricted operational windows. The use of magnetic perturbations to suppress and mitigate ELMs has been shown in a number of devices [13–15], but this requires robust, resilient, likely in-vessel coils for future devices. Finally, the Enhanced *D*-alpha *H* mode [16] and Type II ELMy *H* mode [17] may have acceptably small ELM transients, but these also appear in narrow operational windows. The completely ELM-free regime has also been obtained in the National Spherical Torus Experiment (NSTX) following conventional lithium (Li) evaporation onto the PFCs, but usually terminated by large ELMs, leading to a rapid accumulation of impurities [10,18]. This offers an attractive solution but maybe not enough for future tokamaks beyond the next generation fusion machines like ITER and DEMO, which will need a reliable method for controlling or suppressing large ELMs [19].

This Letter reports, for the first time, the achievement of a long-pulse *H* mode with a record ELM-free period lasting ~18 s, about 450 times the energy confinement time, in the Experimental Advanced Superconducting Tokamak (EAST), by real-time injection of a Li aerosol into the edge plasma, which actively suppresses ELM formation

and prevents impurity accumulation. What is truly remarkable is that Li aerosol injection promotes the growth of an edge coherent mode (ECM), which provides continuously heat and particle exhaust, thus preventing impurity accumulation and facilitating steady-state *H*-mode operation with a long ELM-free period. This is attributed to the increase in edge plasma collisionality arising from the presence of Li at the edge, as predicted by the GYRO code.

Our results differ from and extend the previous NSTX results where lithium was used to suppress ELMs in two principal ways. (1) NSTX observed a reduction in recycling and edge transport and turbulence [20,21], with the reduced recycling at the wall playing a central role. Our results show instead an increase of edge turbulence, which is directly manipulated via active Li injection; the role of the wall does not appear to be central. (2) In the NSTX work, the improvement of particle confinement was too good, in that impurity and hence radiated power ramped with time, leading to relatively short nonsteady *H* modes. Here, the increase in fluctuations appears to increase particle transport sufficiently to prevent impurity accumulation for many hundreds of confinement times.

EAST (major and minor radii of 1.85 and 0.45 m, respectively) was built to demonstrate long-pulse high-performance *H*-mode plasmas with ITER-like configuration and heating schemes [22]. To facilitate long-pulse operation on EAST, we have developed an advanced wall conditioning technique with Li by coupling Li evaporation into ion cyclotron resonance frequency (ICRF) wave-assisted plasma discharges [23], as well as real-time injection of a fine Li aerosol (“Li dropper”) in collaboration with PPPL [24]. Using a Li dropper, real-time Li aerosol injection during plasma operation on walls precoated with lithium between discharges is expected to repair and replenish the initial Li coating; this combination has suppressed ELMs to obtain a long pulse ELM-free *H* mode. Using a resonating piezoelectric disk with a central aperture, the dropper injects an evaporating Li aerosol (droplet diameter  $\sim 45 \mu\text{m}$ ) into the plasma scrape-off layer by simply dropping spherical Li granules in a controlled manner [25]. The Li aerosol can be reproducibly injected in EAST through the upper divertor gap in *H*-mode discharges with an adjustable flow rate of 30–60 mg/s. During the discharges studied in this work, a Li aerosol was injected directly into the plasma upper *X* point at  $\sim 2 \times 10^6$  spheres/s,  $\sim 4 \times 10^{21}$  atoms/s, as shown in Fig. 1. The location of the aerosol injector with the downward trajectory of injected Li particles and the sequence of true color images of Li evaporating, ionizing, and being transported are shown in the diagram. The velocity of the aerosol was about 9 m/s, driven by gravity when contacting the scrape-off layer plasma.

Real-time injection of the Li aerosol facilitates *H*-mode maintenance and enables the plasma to rapidly enter the ELM-free *H*-mode regime with the ELM-free period greatly exceeding the energy confinement time. Figure 2

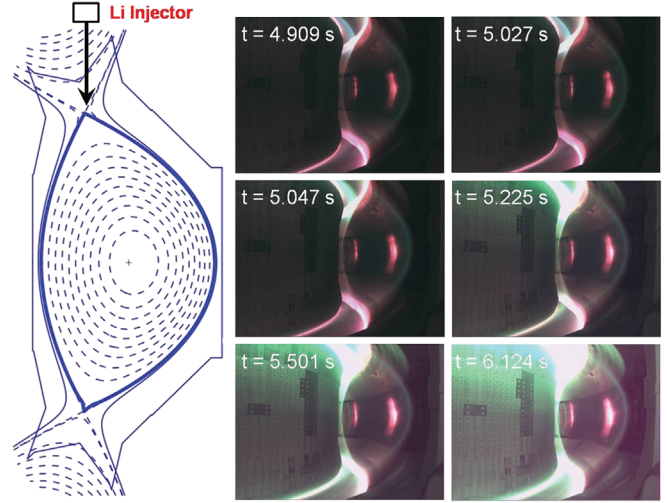


FIG. 1 (color). Left: a magnetic flux plot typical of the double-null discharges (e.g., No. 41079) studied in this work with the location of the Li aerosol injector indicated. Right: a sequence of true color images beginning at the time of Li aerosol injection started at  $\sim 4.9$  s, viewed at a location 90 deg toroidally separated from the injection point. The green color shows 5485 Å Li-II emission from singly-ionized Li, demonstrating that relatively uniform Li emission can be achieved about 1 sec after the start of the Li aerosol injection. It is interesting to note the initial absence of Li-II emission, even though the EAST PFCs were covered with 500 g of evaporated Li accumulated before the start of this Li aerosol injection experiment.

shows the divertor  $D\alpha$  signal near the out strike point in a series of three discharges with Li aerosol injection, shots No. 41075, No. 41078 and No. 41079, along with the discharges before and after Li injection, shot No. 41073

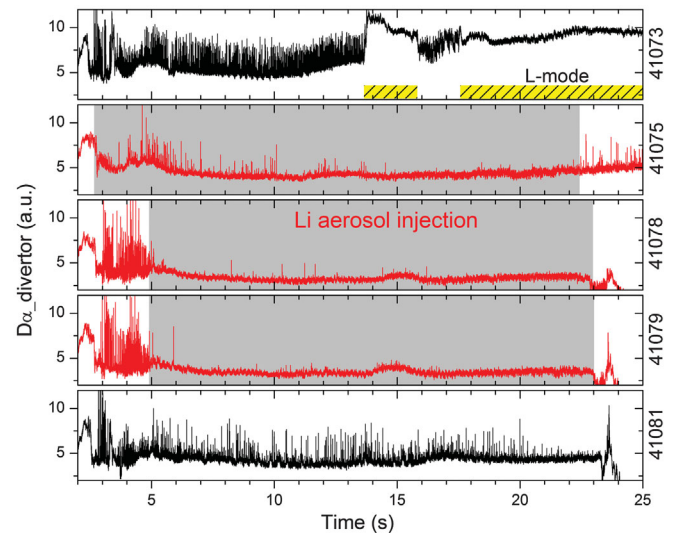


FIG. 2 (color). Demonstration of reproducible long-pulse ELM-free *H* modes with real-time Li injection. Data shown are the evolution of  $D\alpha$  emission at the lower divertor target in various *H*-mode plasmas with and without Li aerosol injection. ELMs are manifested as spikes in the  $D\alpha$  emission.

and shot No. 41081, respectively. The nominal externally controlled discharge parameters for these discharges are as follows: plasma current  $I_p = 0.28$  MA, toroidal magnetic field  $B_T = 1.9$  T, central density  $n_e = 2 \times 10^{19}$  cm $^{-3}$ , central electron temperature  $T_e(0) = 1.2$  keV. Plasmas were in the double-null configuration with elongation  $\delta = 0.5$  and triangularity  $\kappa = 1.7$ . Auxiliary heating power was provided by 0.75 MW of  $H$ -minority ICRF as well as 1.4 MW of lower hybrid wave (LHW) heating. The discharges entered the  $H$  mode at  $\sim 3$  s after plasma breakdown, and attained an  $H$ -mode energy confinement time  $\tau_E \sim 40$  ms, with the  $H$ -mode confinement enhancement factor [26]  $H_{98(y,2)} \sim 0.8$ . As can be seen, in the first discharge with Li injection (No. 41075), the amplitude of the ELMs was significantly reduced and the  $H$  mode was maintained throughout the discharge, in contrast to the discharge prior to Li injection (No. 41073). Subsequently, Li injection quickly resulted in reproducible long-pulse ELM-free  $H$ -mode discharges with a stationary ELM-free phase over the entire duration of Li injection,  $\sim 18$  s, which is about  $450 \times \tau_E$ . When Li injection was switched off (No. 41081), the ELMs reappeared, albeit with small amplitudes, and the discharge remained in the  $H$  mode, presumably benefitting from the Li deposition from the previous discharges.

Contrary to expectations, the plasma density and radiation remains steady during the ELM-free phase, in spite of the absence of ELMs, as shown in Fig. 3. As can be seen, the edge plasma radiation is significantly higher in the discharge with real-time Li injection (No. 41079). However, the radiation at the core plasma is even lower than in the discharge without Li injection (No. 41081). This clearly indicates no impurity accumulation in the core plasma, while the enhanced edge radiation is attributed to the increased Li concentration at the edge, as manifested by strong Li-II emission. In addition, real-time Li injection leads to a pronounced reduction in the baseline (no fluctuating part at the interval of ELMs) of the divertor  $D\alpha$  signal, by  $\sim 50\%$ , representing a significant reduction in neutral recycling taking place at the divertor target plate. This demonstrates that real-time Li injection further reduces divertor recycling compared to conventional Li coating by thermal evaporation [23]. The divertor peak power flux, obtained from the divertor Langmuir probes, is also significantly reduced owing to the absence of ELMs. Note that the peak heat flux during the real-time Li-aerosol induced ELM-free  $H$  mode is much lower than that of the ELMs achieved in EAST with conventional Li wall conditioning [27].

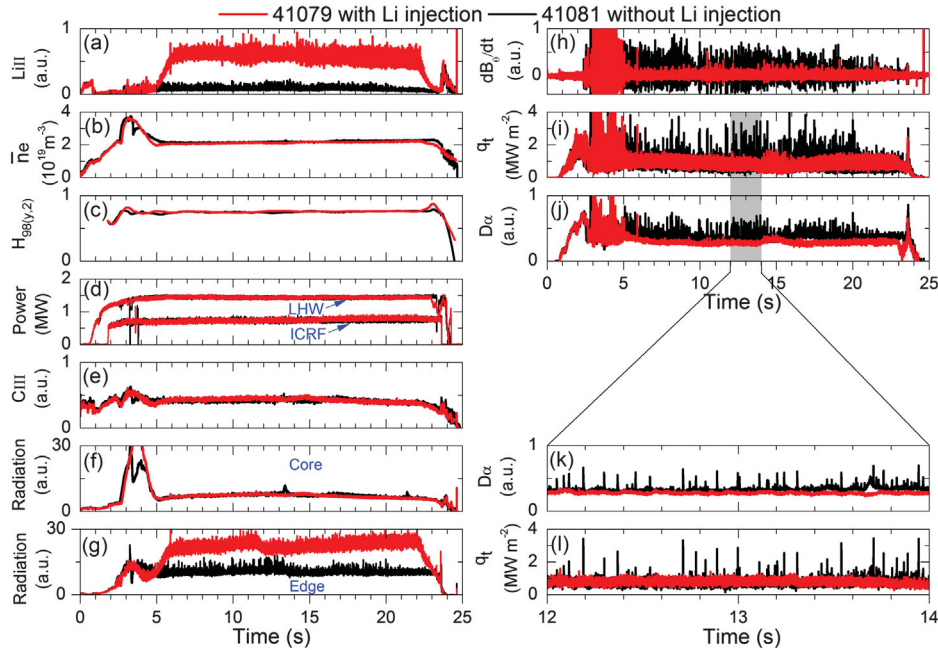


FIG. 3 (color). Comparison of two long-pulse  $H$ -mode discharges with and without real-time Li injection (double null divertor configuration,  $P_{\text{LHW}} = 1.4$  WM,  $P_{\text{ICRF}} = 0.7$  WM). Shown are the (a) Li-II line radiation emission integrated across the main plasma at midplane, (b) line average density, (c)  $H_{98(y,2)}$  confinement enhancement factor, (d) LHW and ICRF heating power, (e) C-III line radiation, (f) core radiation from ultraviolet photodiodes with a wavelength range of 0.2–1240 nm, (g) edge radiation, (h) MHD signals measured by the low-sampling-frequency Mirnov coil (50 kHz) at midplane on the high field side, (i) divertor heat flux measured by Langmuir probes embedded in the lower outboard divertor target, and (j)  $D\alpha$  at the lower outboard divertor. Panels (k) and (l) show an expanded time base of the  $D\alpha$  emission and heat flux at the lower outboard divertor, the latter obtained from Langmuir probe data.



It is interesting to note that real-time Li injection leads to a dramatic drop in the low frequency (0.5–1 kHz) magnetohydrodynamics (MHD) activity, Fig. 3(h). Detailed examination reveals that two active modes appear during the relatively quiescent ELM-free phase, at the frequencies near 35–40 kHz, as shown in Fig. 4. The mode with slightly lower frequency (red bands with a poloidal phase of  $2n\pi + \pi$ ) stays constant during the discharge. What is truly remarkable is that the other mode with a slightly higher frequency (yellow bands) grows rapidly upon Li injection (shots 41075 and 41079), exhibiting a poloidal phase of  $2n\pi + (0.3-0.4)\pi$ , compared to the case without Li injection (shot 41081). This higher-frequency mode with a poloidal wavelength of 10.2 cm in the ion diamagnetic drift direction has been identified as the as the ECM in our previous study [28]. We have demonstrated that the ECM is capable of driving significant cross-field particle and heat transport, leading to the avoidance of large ELMs and the long-pulse sustainment of a stationary *H*-mode pedestal.

Thus, the significant enhancement of the ECM intensity associated with real-time Li injection is very likely the underlying mechanism responsible for the achievement of the long-pulse ELM-free *H* mode. According to the GYRO code simulations, which simulate tokamak turbulence by using an eigenvalue solver in a flux tube domain near the peak gradient region of the EAST pedestal with full gyrokinetic species [28], the growth rate of the ECM strongly depends on the local collisionality, given by Ref. [29]:  $v_e^* = 6.921 \times 10^{-18} q_{95} R n_e Z_{\text{eff}} \ln \Lambda / (T_e^2 \epsilon^{3/2})$ , where  $R$ ,  $Z_{\text{eff}}$ ,  $\ln \Lambda$ ,  $\epsilon$ ,  $n_e$ , and  $T_e$  are the major radius, effective ion charge, Coulomb logarithm, aspect ratio, electron density (in  $\text{m}^{-3}$ ), and electron temperature (in eV), respectively. For the discharges with real-time Li injection, the pedestal  $Z_{\text{eff}}$ , evaluated from the bremsstrahlung radiation signals, and hence collisionality both increase by a factor of 1.3. The carbon III emission remains unchanged, indicating that the difference in  $Z_{\text{eff}}$  is mainly due to the injection of lithium. Thus, the normalized collisionality  $v_e^*$  increases from  $\sim 1.5$  to  $\sim 2.0$  in the pedestal steep gradient region due to the increased Li concentration at the edge, which will in turn lead to an increase of the ECM growth rate by a factor of  $\sim 2.8$ , as shown in Fig. 4(a) in Ref. [28]. This may explain the presence of the strong ECM, as seen by Mirnov probes (Fig. 4), in the long-pulse ELM-free discharges obtained with real-time Li injection.

In summary, we have achieved reproducible steady-state ELM-free *H*-mode discharges with a record duration of 18 s in the EAST superconducting tokamak by using a novel technique with real-time injection of a Li aerosol. This long-pulse ELM-free *H* mode is accompanied by a strong ECM, which provides a continued exhaust of energy and particles to maintain the *H*-mode pedestal in the absence of ELMs, without impurity accumulation in the confined plasma. GYRO modeling shows that real-time Li injection further enhances the growth rate of the ECM due

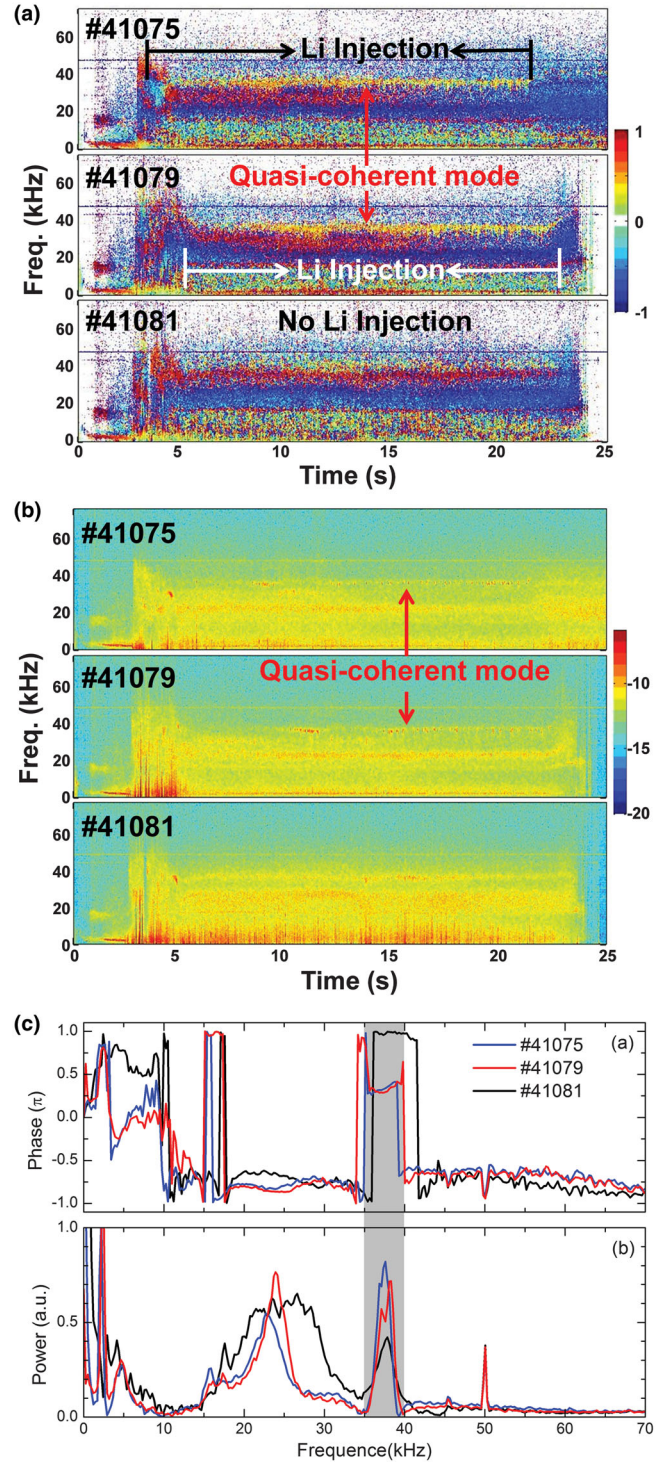


FIG. 4 (color). The magnetic fluctuation time-frequency spectrum with two active edge coherent modes at 35–40 kHz in *H*-mode plasmas with  $q_{95} = 7.4$  using real-time Li aerosol injection. Shown are the (a) phase spectrum, obtained from two high-sampling-frequency (250 kHz) Mirnov magnetic pickup probes near the midplane on the outboard side (the poloidal distance is 63 cm; the intensity scale from  $-1$  to  $1$  means the poloidal phase from  $2n\pi - \pi$  to  $2n\pi + \pi$ ), (b) power intensity spectrum, obtained from one of the above probes, and (c) phase and power intensity versus frequency at 20 s during the shots.

to the increase in  $Z_{\text{eff}}$  at the  $H$ -mode pedestal, arising from the increased Li concentration at the edge. These novel results demonstrate a new way to achieve steady-state  $H$ -mode plasmas and provide a promising approach towards steady-state high-performance plasma operation for future fusion devices.

This work was supported by the National Magnetic Confinement Fusion Science Program of China under Contracts No. 2013GB114004 and No. 2011GB107000, and National Nature Science Foundation of China under Contracts No. 11321092 and No. 11405210, and Chinese academy of sciences visiting professorship for senior international scientists under Contracts No. 2012T1J0025.

---

\*Corresponding author.  
hujs@ipp.ac.cn

- [1] J. Li, H. Y. Guo *et al.*, A long-pulse high-confinement plasma regime in the experimental advanced superconducting tokamak, *Nat. Phys.* **9**, 817 (2013).
- [2] E. Tsitrone, Key plasma wall interaction issues towards steady state operation, *J. Nucl. Mater.* **363–365**, 12 (2007).
- [3] A. Loarte *et al.*, Chapter 4: Power and particle control, *Nucl. Fusion* **47**, S203 (2007).
- [4] P. T. Lang *et al.*, ELM control strategies and tools: status and potential for ITER, *Nucl. Fusion* **53**, 043004 (2013).
- [5] H. Zohm, Edge localized modes (ELMs), *Plasma Phys. Controlled Fusion* **38**, 105 (1996).
- [6] J. W. Connor, A review of models for ELMs, *Plasma Phys. Controlled Fusion* **40**, 191 (1998).
- [7] Y. Liang *et al.*, Magnetic Topology Changes Induced by Lower Hybrid Waves and their Profound Effect on Edge-Localized Modes in the EAST Tokamak, *Phys. Rev. Lett.* **110**, 235002 (2013).
- [8] R. Maingi, Enhanced confinement scenarios without large edge localized modes in tokamaks: Control, performance, and extrapolability issues for ITER, *Nucl. Fusion* **54**, 114016 (2014).
- [9] D. K. Mansfield *et al.*, Transition to ELM-free improved H-mode by lithium deposition on NSTX graphite divertor surfaces, *J. Nucl. Mater.* **390–391**, 764 (2009).
- [10] R. Maingi *et al.*, Continuous Improvement of H-Mode Discharge Performance with Progressively Increasing Lithium Coatings in the National Spherical Torus Experiment, *Phys. Rev. Lett.* **107**, 145004 (2011).
- [11] C. M. Greenfield *et al.*, Quiescent Double Barrier Regime in the DIII-D Tokamak, *Phys. Rev. Lett.* **86**, 4544 (2001).
- [12] K. H. Burrell, T. Osborne, P. Snyder, W. West, M. Fenstermacher, R. Groebner, P. Gohil, A. Leonard, and W. Solomon, Quiescent H-Mode Plasmas with Strong Edge Rotation in the Cocurrent Direction, *Phys. Rev. Lett.* **102**, 155003 (2009).
- [13] T. E. Evans *et al.*, Suppression of Large Edge-Localized Modes in High-Confinement DIII-D Plasmas with a Stochastic Magnetic Boundary, *Phys. Rev. Lett.* **92**, 235003 (2004).
- [14] W. M. Suttrop *et al.*, First Observation of Edge Localized Modes Mitigation with Resonant and Nonresonant Magnetic Perturbations in ASDEX Upgrade, *Phys. Rev. Lett.* **106**, 225004 (2011).
- [15] Y. M. Jeon *et al.*, Suppression of Edge Localized Modes in High-Confinement KSTAR Plasmas by Nonaxisymmetric Magnetic Perturbations, *Phys. Rev. Lett.* **109**, 035004 (2012).
- [16] M. Greenwald *et al.*, Characterization of enhanced  $D\alpha$  high-confinement modes in Alcator C-Mod, *Phys. Plasmas* **6**, 1943 (1999).
- [17] J. Stober, M. Maraschek, G. D. Conway, O. Gruber, A. Herrmann, A. C. C. Sips, W. Treutterer, H. Zohm, and ASDEX Upgrade Team, Type II ELMy H modes on ASDEX Upgrade with good confinement at high density, *Nucl. Fusion* **41**, 1123 (2001).
- [18] H. W. Kugel *et al.*, The effect of lithium surface coatings on plasma performance in the National Spherical Torus Experiment, *Phys. Plasmas* **15**, 056118 (2008).
- [19] ITER Physics Basis Editors, ITER Physics Expert Group Chairs, and Co-Chairs, and ITER Joint Central Team, and Physics Integration Unit, Chapter 1: Overview and summary, *Nucl. Fusion* **39**, 2137 (1999).
- [20] R. Maingi *et al.*, Edge-Localized-Mode Suppression through Density-Profile Modification with Lithium-Wall Coatings in the National Spherical Torus Experiment, *Phys. Rev. Lett.* **103**, 075001 (2009).
- [21] J. M. Canik *et al.*, Edge transport and turbulence reduction with lithium coated plasma facing components in the National Spherical Torus Experiment, *Phys. Plasmas* **18**, 056118 (2011).
- [22] B. Wan, J. Li, H. Guo, Y. Liang, and G. Xu, Progress of long pulse and H-mode experiments in EAST, *Nucl. Fusion* **53**, 104006 (2013).
- [23] G. Z. Zuo, J. S. Hu, J. G. Li, Z. Sun, D. K. Mansfield, and L. E. Zakharov, Lithium coating for H-mode and high performance plasmas on EAST in ASIPP, *J. Nucl. Mater.* **438**, S90 (2013).
- [24] G. Z. Zuo, J. S. Hu, S. Zhen, J. G. Li, D. K. Mansfield, B. Cao, J. H. Wu, and L. E. Zakharov, Comparison of various wall conditionings on the reduction of H content and particle recycling in EAST, *Plasma Phys. Controlled Fusion* **54**, 015014 (2012).
- [25] D. K. Mansfield, A. L. Roquemore, H. Schneider, J. Timberlake, H. Kugel, and M. G. Bell, A simple apparatus for the injection of lithium aerosol into the scrape-off layer of fusion research devices, *Fusion Eng. Des.* **85**, 890 (2010).
- [26] E. J. Doyle *et al.*, Chapter 2: Plasma confinement and transport, *Nucl. Fusion* **47**, S18 (2007).
- [27] L. Wang *et al.*, Characterizations of power loads on divertor targets for type-I, compound and small ELMs in the EAST superconducting tokamak, *Nucl. Fusion* **53**, 073028 (2013).
- [28] H. Q. Wang *et al.*, New Edge Coherent Mode Providing Continuous Transport in Long-Pulse H-mode Plasmas, *Phys. Rev. Lett.* **112**, 185004 (2014).
- [29] O. Sauter, C. Angioni, and Y. R. Lin-Liu, Neoclassical conductivity and bootstrap current formulas for general axisymmetric equilibria and arbitrary collisionality regime, *Phys. Plasmas* **6**, 2834 (1999).